Simple model for convective free boundary mass transfer inside a square capillary tube

DAMELYS ZABALA* , AURA L. LÓPEZ DE RAMOS**
*CIMEC, Escuela de Ingeniería Mecánica, **Departamento de Termodinámica y Fenómenos de Transferencia
*Universidad de Carabobo, **Universidad Simón Bolívar
* Av. Universidad, Edf. Facultad de Ingeniería, Bárbula, Estado Carabobo, **Apartado Postal 89.000, Caracas VENEZUELA

Abstract: - In a previous work[1], moving boundary mass transfer inside a cylindrical capillary tube was properly modeled considering variable diffusion coefficient and no convective effects in the liquid phase. The numerical solution was semi-explicit because inside the finite difference matrix, the terms associated to the diffusion coefficients depend on the solute concentration. In the other hand, experimental results in that work showed such model it is not adequate to represent the mass transfer inside square capillaries, because convective flow patterns generated by square tube corners were not considered in the mass transfer model. In this work, the convective term was considered in the liquid phase and in the interface equations. The technique for solving the model was based in the methodology developed by Illingworth and Golosnoy [2] which allowed solute conservation and transformed the moving boundaries in fixed ones. Discretisation in liquid phase and interface equations was modified due the inclusion of the new term. Results showed that the experimental interface position inside the square glass capillary tube was well represented by this numerical model with convective effects. Simulation time (10 min) in this model is similar to the simulation time in the previous no convective model.

Key-Words: - Square capillary, Free boundary, Mass transfer, Numerical Modeling, Diffusion

1 Introduction

Fluid displacement inside polygonal capillary tubes or cells has been studied trying to understand fluid-solid interactions in porous media [3-7]. Corners of capillary tubes promote fluid movement by a liquid filament which rises along the crevice. Corners are considered equivalent for simulation of the effects of active capillary surfaces in porous media[8,9]. Enhanced oil recovery is one of the applications of interest of these studies, with immiscible [10-11] or miscible displacement [12-17]. In this work, experiments with carbon dioxide diffusing in a liquid hydrocarbon were done, with both fluids contained in square and cylindrical glass capillary tubes. Experimental gas-liquid interface positions at the center of the tube were observed and it was found that the interface moves faster inside the square capillary tube. A model of this miscible displacement it is necessary to determine the contribution of the corner presence to an improved mass transfer process like the miscible CO_2 injection in hydrocarbons. In this model, one-dimension displacement was considered to simplify the geometric problem involved with the liquid filament shape.

2 Problem Formulation

2.1 Mathematical Model

For a component "i", one-dimension continuity equations for liquid and gas phases are: [2,18,19]

$$\frac{\partial C_{i,L}}{\partial t} + \frac{\partial N_{i,L}}{\partial z} = 0 \quad , 0 \le z \le s(t) \tag{1}$$

$$\frac{\partial C_{i,G}}{\partial t} + \frac{\partial N_{i,G}}{\partial z} = 0 \quad , s(t) \le z \le L \tag{2}$$

Total flux N can be related to the diffusive flux J [18,19]:

$$J_i = C_i U_i - C_i U^{ref} = N_i - C_i U^{ref} \tag{3}$$

The reference velocity for the phase (U^{ref}) can be defined in different ways. A possibility is the average molar velocity, and for a binary mixture "i,j" can be expressed by:

$$U^{molar} = \frac{\sum C_j U_j}{C} = \frac{C_i U_i + C_j U_j}{C} = \frac{N_i + N_j}{C} \tag{4}$$

Replacing equation (4) in equation(3), and defining the diffusive flux with the Fick law:

$$J_i = N_i - x_i\left(N_i + N_j\right) = -D_i \frac{\partial C_i}{\partial z} \qquad (5)$$

The flux of the "j"component can be related to the flux of the "i"component.

$$N_j = \alpha N_i \qquad (6)$$

Value of α, define convective term in continuity equation. For α=0, it is diffusion of "i" in a stagnant fluid "j". For α= -1, it is equimolar counterdiffusion and it is numerical equivalent of no convective effect case. Combining equations (5) and (6):

$$N_i = \frac{-D_i}{1 - x_i(1+\alpha)} \frac{\partial C_i}{\partial z} = \frac{-D_i}{\beta} \frac{\partial C_i}{\partial z} \qquad (7)$$

For carbon dioxide, one-dimension continuity equations for liquid and gas phases are: [1,9]

$$\frac{\partial x_C}{\partial t} = \frac{\partial}{\partial z}\left(\frac{D_L}{\beta}\frac{\partial x_C}{\partial z}\right) \quad , 0 \le z \le s(t) \qquad (8)$$

$$\frac{\partial y_C}{\partial t} = D_G \frac{\partial^2 y_C}{\partial z^2} \quad , \quad s(t) \le z \le L \qquad (9)$$

Equations (8) and (9) are for mass transfer process with constant phase densities and without chemical reaction. Equation (8) includes convective effects. The initial and boundary conditions are in Table 1. Making a mass balance for carbon dioxide across the moving interface, its position can be determined by solving the ordinary differential equation (10). [2,20, 21]

$$C_L \frac{D_L}{\beta}\frac{\partial x_C}{\partial z}\bigg|_{z=s(t)^-} - C_G D_G \frac{\partial y_C}{\partial z}\bigg|_{z=s(t)^+} = \left(y_C^{sat} C_G - x_C^{sat} C_L\right)\frac{ds(t)}{dt}, \qquad z = s(t) \qquad (10)$$

Following the methodology developed by Illingworth and Golosnoy[2], the moving boundaries are transformed in fixed ones, by definition of new spatial variables *u* and *v*. The concentrations are defined by new dependant variables *p* and *q*.

$$u = \frac{z}{s(t)}, \quad v = \frac{z - s(t)}{L - s(t)}$$

$$p(u,t) = x_C(z,t), \quad q(v,t) = y_C(z,t)$$

Table 1. Initial and border conditions

Gas phase	Liquid phase
$t = 0, \quad y_C = y_C^{ini}$	$t = 0, \quad x_C = x_C^{ini}$
$z = s(t), \quad y_C = y_C^{sat}$	$z = s(t), \quad x_C = x_C^{sat}$
$z = L, \quad y_C = y_C^{ini}$	$z = 0, \quad \frac{\partial x_C}{\partial z} = 0$

The transformed equations inside the phases are (11) and (12), and their respective transformed initial and boundary conditions are in Table 2.

$$\frac{\partial p}{\partial t} - V\frac{u}{s}\frac{\partial p}{\partial u} = \frac{\partial}{\partial u}\left(\frac{D_L}{\beta s^2}\frac{\partial p}{\partial u}\right) \quad , 0 \le u \le 1 \qquad (11)$$

$$\frac{\partial q}{\partial t} - V\frac{1-v}{L-s}\frac{\partial q}{\partial v} = \frac{\partial}{\partial v}\left(\frac{D_G}{(L-s)^2}\frac{\partial q}{\partial v}\right), 0 \le v \le 1 \qquad (12)$$

Table 2. Transformed initial and border conditions

Gas phase	Liquid phase
$t = 0, \quad q = y_C^{ini}$	$t = 0, \quad p = x_C^{ini}$
$v = 0, \quad q = y_C^{sat}$	$u = 1, \quad p = x_C^{sat}$
$v = 1, \quad q = y_C^{ini}$	$u = 0, \quad \frac{\partial p}{\partial u} = 0$

The transformed interface equation is:

$$C_L \frac{D_L}{\beta s}\frac{\partial p}{\partial u}\bigg|_{u=1} - C_G \frac{D_G}{L-s}\frac{\partial q}{\partial v}\bigg|_{v=0} = \left(y_C^{sat} C_G - x_C^{sat} C_L\right)\frac{ds(t)}{dt}, \qquad u = 1, \; v = 0 \qquad (13)$$

The interface equation (13) is converted to an expression which conserves solute [2].

$$\frac{\partial}{\partial t}\left\{s(t) C_L \int_0^1 p(u,t)du + \left(L - s(t)\right) C_G \int_0^1 q(v,t)dv\right\} = 0 \qquad (14)$$

For discretisation, the liquid phase equation is written in a divergent form, eq.(15) , and it is integrated, eq. (16), between the indicated *u* and *t* intervals, defined according equation (17).

$$\frac{\partial}{\partial t}(ps) = \frac{\partial}{\partial u}\left(Vpu + \frac{D_L}{\beta s}\frac{\partial p}{\partial u}\right) \qquad (15)$$

After the first integration equation (16) is transformed in eq. (18). For the second integration, these are the considerations. For the left side of eq.(18), *p* is considered constant for the *u* integration

interval.

$$\int_{u_{i-1/2}}^{u_{i+1/2}}\int_{t^j}^{t^{j+\sigma}} \frac{\partial}{\partial t}(ps)\,dtdu = \int_{t^j}^{t^{j+\sigma}}\int_{u_{i-1/2}}^{u_{i+1/2}} \frac{\partial}{\partial u}\left(Vpu + \frac{D_L}{\beta s}\frac{\partial p}{\partial u}\right)dudt$$

(16)

$$u_{i+1/2} = \frac{u_i + u_{i+1}}{2}; \quad u_{i-1/2} = \frac{u_i + u_{i-1}}{2} \tag{17}$$

$$\int_{u_{i-1/2}}^{u_{i+1/2}} \left\{ p^{j+1}s^{j+1} - p^j s^j \right\} du =$$

$$\int_{t^j}^{t^{j+1}} \left\{ \begin{array}{l} \left(Vp_{i+1/2}u_{i+1/2} + \dfrac{(D_L)_{i+1/2}}{\beta_{i+1/2}s}\left.\dfrac{\partial p}{\partial u}\right|_{i+1/2} \right) \\ -\left(Vp_{i-1/2}u_{i-1/2} + \dfrac{(D_L)_{i-1/2}}{\beta_{i-1/2}s}\left.\dfrac{\partial p}{\partial u}\right|_{i-1/2} \right) \end{array} \right\} dt \tag{18}$$

For the right side of eq.(18), *p* and other time functions are considered constant for the *t* integration interval defining the parameter σ (0≤σ≤1). This constant value is defined according eq. (19).

$$p_i^{j+\sigma} = \sigma p_i^{j+1} + (1-\sigma)\, p_i^j \tag{19}$$

$$\frac{p_i^{j+1}\left[\left(r_{i+1/2}^{j+1}\right) - \left(r_{i-1/2}^{j+1}\right)\right] - p_i^j\left[\left(r_{i+1/2}^{j}\right) - \left(r_{i-1/2}^{j}\right)\right]}{\left(t^{j+1} - t^j\right)} =$$

$$\left\{ \begin{array}{l} \left[V^{j+\sigma} p_{i+1/2}^{j+\sigma} u_{i+1/2} + \dfrac{(D_L)_{i+1/2}^{j+\sigma}}{\beta_{i+1/2}^{j+\sigma} s^{j+\sigma}}\left.\dfrac{\partial p}{\partial u}\right|_{i+1/2}^{j+\sigma} \right] \\ -\left[V^{j+\sigma} p_{i-1/2}^{j+\sigma} u_{i-1/2} + \dfrac{(D_L)_{i-1/2}^{j+\sigma}}{\beta_{i-1/2}^{j+\sigma} s^{j+\sigma}}\left.\dfrac{\partial p}{\partial u}\right|_{i-1/2}^{j+\sigma} \right] \end{array} \right\} \tag{20}$$

$$r_{i\pm 1/2}^j = s^j u_{i\pm 1/2} \tag{21}$$

Equation (20) is the general finite difference scheme for the liquid phase, except for the border points. This scheme will be fully implicit when σ=1.

Figure 1 shows a scheme of the mass transfer process with a flat interface: this mathematical model in one dimension does not consider the real shape of the interface, with a meniscus and the filaments in the corners of the tube.(Fig.2)

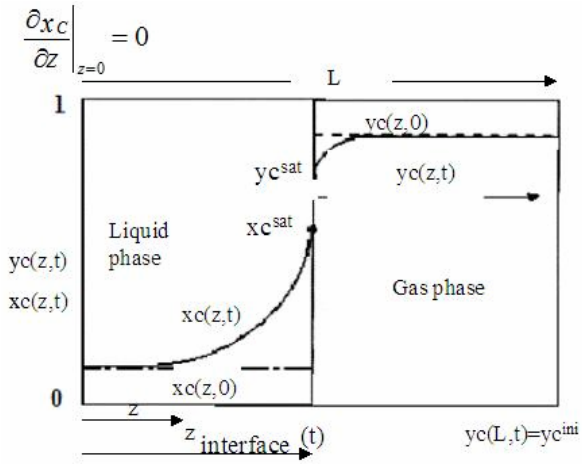

Fig. 1. Mass transfer process illustration.

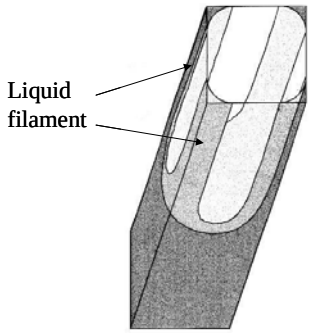

Fig. 2. Liquid filament rise illustration.

2.2 Experimental Equipment

A visualization cell is built, with two plexiglas caps and four common glass walls. The capillary tube is fixed to brass connectors in upper and lower extremes of the cell using epoxy glue (Fig.3). The space between the capillary and the cell walls is filled with glycerol (99.5%) which has the same refractive index than the glass, to avoid distortion by light diffraction. In the capillary lower extreme, a membrane is inserted between the tube and the brass connector to seal this side during the test. The hydrocarbon (n-C10: n-Decane) is injected by this extreme, passing a syringe through a small hole in the connector and penetrating the membrane. After n-C10 injection, the syringe is removed. The carbon dioxide is injected through the upper side at 23.5 ºC and 1480 kPa (abs) and the recording process begins. The camcorder is a Sony mini DV, model DCR-HC42 with a 12X macro lens, positioned in a way that the meniscus can be

observed between the marks on the capillary (Fig. 4). The space between marks is 5 mm, so it is possible to have the calibration pixel/mm direct from the test images. Capillary tube data can be found in [1].

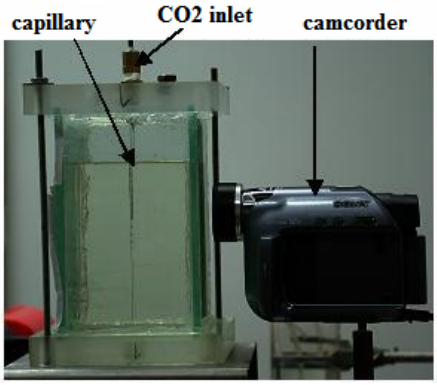

Fig.3. Visualization cell

3 Problem Solution

3.1 Mathematical Model Results

Diffusion coefficients are considered variable in liquid phase and constant in gas phase. D_L is estimated by Caldwell and Babb [22] equation using Scheibel correlation [23] for dilute solution CO_2 diffusion coefficient. The term for the dilute solution n-C10 diffusion coefficient was neglected (Eq.(22)).

$$D_L = (1-p)\, D_C^{dil}\left[1 - p\frac{2A}{RT}(1-p)\right] \qquad (22)$$

The thermodynamic factor is calculated using activity coefficient estimated by Margules with two subscripts and the A parameter for this model was determined [1,24]. D_G is calculated by Wilke and Lee correlation [25]. C_G is approximated to pure CO_2 molar density which it is calculated by Pitzer and Sterner equation of state [26]. Calculated and experimental data are shown in Table 3.

Table 3. Data at P=1480 kPa (abs), T=23.5 ºC

y_C^{sat}	0.9994 [27]	D_G [mm^2/h]	2.125.10^3
y_C^{ini}	1	A [kJ/kmol]	7900 [1]
x_C^{sat}	0.1884 [27]	C_G [mol/mm^3]	0.651.10^{-6}
x_C^{ini}	0	C_L [mol/mm^3]	2.19. 10^{-6} [1]

The partial derivative equation system(11), (12) and (14) is discretised and numerically solved by finite difference method. The algorithms used are of first order accuracy. The space discretisation is done with a fixed mesh for gas phase and with three different step sizes for liquid phase, the smallest one near the interface. The time discretisation is done with two different time step sizes, because very small time step improves the solution stability but increases the simulation time as it was found when the no convective model was solved [28]. The finite difference solution scheme is semi-implicit, because the concentration terms present in the liquid phase for D_L and β are evaluated in the previous time (σ =0) in order to have a constant coefficient matrix. All the other concentration terms are evaluated in the present time (σ =1).

3.2 Experimental Results

Square capillary experimental interface positions are shown in figure 4.

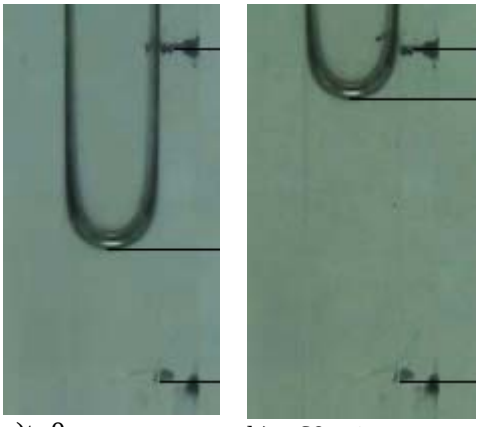

a)t=0 b)t=60 min

Fig.4. Displacement inside square capillary

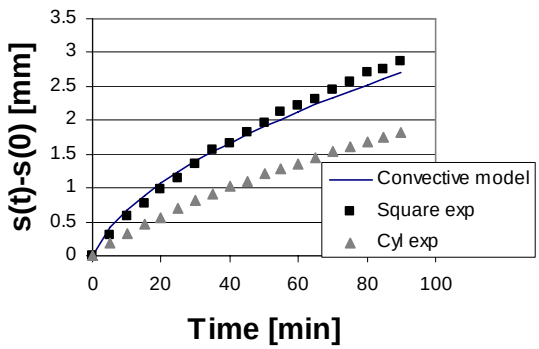

Fig.5. Experimental and theoretical result comparison

The experimental results for interface displacement relative to its initial position are compared with the results predicted by the mathematical model as it is shown in Fig. 5. Interface displacement for square capillaries is larger than the displacement for cylindrical ones. This behavior is similar to the reported by other authors, in experiments done at

different temperature and pressure and with other saturated hydrocarbons [9,15-17]. Also, Fig. 5 shows that the convective model result represents the interface displacement inside the square capillary in a satisfactory way. The average relative error between the model and the square experimental results is 7.53%, obtained by adjustment of the parameter α= 2.98, with the square capillary experimental data. Simulation time is 10 min, the same for the previous model with no convective effects [1].

4 Conclusion

A simplified mass transfer model, which considers both variable diffusion coefficient and convective effects in the liquid phase and constant density for both phases, is adequate to represent CO_2 diffusion process in liquid n-C10, inside a square capillary tube. This model can be improved if the momentum equation for liquid phase is considered coupled with the mass transfer equation.

List of Symbols

C_j= molar density of "j" phase, [mol/mm^3].
D_j= CO_2 diffusion coefficient in "j" phase, [mm^2/h].
D_C^{dil} =dilute solution CO_2 diffusion coefficient, [mm^2/h].
J= Molar diffusive flux, [mol/(mm^2 h)]
L= capillary tube lenght, [mm].
N= Molar total flux, [mol/(mm^2 h)]
P= absolute pressure, [kPa]
R= 8.3144 kJ/kmol K
s=s(t)= interface position, relative to capillary tube bottom [mm].
$V = ds(t)/dt$ = interface velocity,[mm/h].
T= temperature, [K]
x_C= CO_2 molar fraction in liquid phase, [-].
y_C= CO_2 molar fraction in gas phase, [-].

Greek letters

α = molar flux ratio hydrocarbon/CO_2= N_H/N_C, [-]

Subscripts	*Superscripts*
L= liquid phase	ini= initial
G= gas phase	sat= saturation

Acknowledgement

The authors want to thank CDCH-Universidad de Carabobo (I.M. Nº 0135-06), Fonacit (S1-2001-000778) and OPSU-Proyecto Alma Mater for their financial support.

References:

[1] Zabala, D.; López de Ramos, A. Gas-Liquid Interface Displacement: Numerical and experimental comparative analysis for carbon dioxide diffusion into n-decane. Paper 538-229, presented at *4th IASME / WSEAS Int. Conf. on Fluids Mechanics and Aerodynamics*, Crete, Greece, Aug. 21-23, 2006.

[2] Illingworth, T.C.; Golosnoy, I.O. Numerical solutions of diffusion-controlled moving boundary problems which conserve solute. *Journal of Computational Physics*, Vol. 209, N1, 2005, pp. 207-225.

[3] Lenormand, R.; Zarcone, C. Role of roughness and edges during imbibition in square capillaries. Paper SPE 13264, presented at the *59th Annual Technical Conference and Exhibition of the Society of Petroleum Engineers of AIME*, Houston, Texas, Sept. 16-19, 1984.

[4] Patzek, T.W.; Kristensen, J.G. Shape Factor and Hydraulic Conductance in Noncircular Capillaries I: One-Phase Creeping Flow. *J. of Colloid and Interface Science*, Vol. 236, 2001, pp.295-304.

[5] Patzek, T.W.; Kristensen, J.G. Shape Factor Correlations of Hydraulic Conductance in Noncircular Capillaries II: Two-Phase Creeping Flow. *J. of Colloid and Interface Science*, Vol. 236, 2001, pp.305-317.

[6] Simmons, M.; Wong, D.; Travers, P.; Rothwell, J. Bubble Behaviour in Three Phase Capillary Microreactors. *International Journal of Chemical Reactor Engineering*, Vol 1, 2003, A30.

[7] Patrick, R. Jr.; Klindera, T.; Crynes, L.L., Cerro, R.L. y Abraham, M.A. Residence time distribution in three-phase monolith reactor. *AIChE Journal*, Vol. 41, 2004, 649-657.

[8] Concus, P.; Finn, R. On the behavior of a capillary surface in a wedge. *Proceeding of the National Academy of Science*, 63, 1969.

[9] López de Ramos, A. *Capillary enhanced diffusion of CO_2 in porous media*. Ph.D. Dissertation, University of Tulsa, 1993.

[10] Firincioglu, T.; Blunt, M.; Zhou, D. Three-phase flow and wettability effects in triangular capillaries. *Colloids and Surfaces A*, Vol. 155, 1999, pp.259-276.

[11] Zhou, D.; Blunt, M. y Orr, F. Jr. Hydrocarbon Drainage along Corners of Noncircular Capillaries. *J. of Colloid and Interface Science*, Vol. 187, 1997, pp.11-21.

[12] Grogan, A.; Pinczewski, V. The role of molecular diffusion processes in tertiary carbon dioxide flooding. Paper SPE/DOE 12706, presented at *SPE/DOE Fourth Joint Symposium on Enhanced Oil Recovery*, Tulsa, OK, Apr. 15-18, 1984.

[13] Campbell, B.; Orr, F. Flow visualization for CO_2/crude oil displacements. *Society of Petroleum Engineers Journal*, 1985, pp.665-678.

[14] Grogan, A.; Pinczewski, V.; Ruskauff, G.; Orr, F. Diffusion of carbon dioxide at reservoir conditions: Models and Measurements. Paper SPE/DOE 14897, presented at *SPE/DOE Fifth Symposium on Enhanced Oil Recovery*, Tulsa, OK, Apr. 20-23, 1986

[15] Aguilera, M.E.; Cerro, R.L and López de Ramos, A. Enhanced CO_2 diffusion in wedges. *Chem. Eng. J.* Vol. 87, 2002, pp. 31-40.

[16] Garrido, A. *Estudio Teórico Experimental de la Transferencia de Masa en Líquidos Confinados en Regiones con Angularidades*. M.Sc Thesis, Universidad Simón Bolívar, 2005.

[17] De Freitas, A. *Estudio del efecto de las esquinas en la transferencia de masa en medios porosos*. M.Sc Thesis, Universidad Simón Bolívar, 2005.

[18] Hines, A.; Maddox, R. *Transferencia de Masa: Fundamentos y Aplicaciones.* Prentice Hall, 1987.

[19] Bejan, A. *Heat Transfer*. John Wiley & Sons, 1995.

[20] Unlusu, Betul; Sunol, Aydin K. Modeling of equilibration times at high pressure for multicomponent vapor-liquid diffusional processes. *Fluid Phase Equilibria*. Vol. 226, 2004, pp. 15-25.

[21] Sassi, M.; Raynaud, M. Solution of the moving-boundaries problems. *Numerical Heat Transfer Part B*, Vol.34, 1998, pp.271-286.

[22] Caldwell C.S.; Babb, A.L. Diffusion in ideal binary liquid mixtures. *J. Phys. Chem*. Vol. 60, 1956, pp 51-56.

[23] Scheibel, E.G. *Ind.Eng.Chem.* Vol.46, 1954, pp. 2007.

[24] Prausnitz, J.; Lichtenthaler, R. y Gomes, E. *"Termodinámica Molecular de los Equilibrios de Fases"*. Prentice Hall, 2000.

[25] Wilke, C.; Lee. *Ind.Eng.Chem.* Vol.47, 1955, pp.1253.

[26] Pitzer, K.S.; Sterner, S.M. Equations of state valid continuously from zero to extreme pressures for H_2O and CO_2. *J.Chem.Phys*. Vol. 101 (4), 1994, pp. 3111-3116.

[27] Reamer, H.; Sage, B. Phase equilibria in hydrocarbon systems. Volumetric and phase behavior of the n-decane-CO_2 system. *J.Chem.Eng.Data*. Vol. 8, 1963, pp. 508-513.

[28] Zabala, D.; López de Ramos, A. Solute concentration effect in gas-liquid interface displacement modeling. *WSEAS Transactions on Fluid Mechanics.* Vol. 1, Nº 6, 2006, pp. 686-691.